Bioorganic & Medicinal Chemistry 19 (2011) 1714–1720

Contents lists available at ScienceDirect

Bioorganic & Medicinal Chemistry

journal homepage: www.elsevier.com/locate/bmc

Structure based design of heat shock protein 90 inhibitors acting as anticancer agents

Munikumar Reddy Doddareddy [a,c], Dhanaji Achyutrao Thorat [a,c], Seon Hee Seo [a], Tae-Joon Hong [b], Yong Seo Cho [a], Ji-Sook Hahn [b], Ae Nim Pae [a,*]

[a] Neuro-Medicine Center, Korea Institute of Science and Technology, PO Box 131, Cheongryang, Seoul 130-650, Republic of Korea
[b] School of Chemical and Biological Engineering, Seoul National University, Sillim-dong, Gwanak-gu, Seoul 151-744, Republic of Korea
[c] School of Science, Korea University of Science and Technology, 52 Eoeun dong,Yuseong-gu, Daejeon 305-333, Republic of Korea

ARTICLE INFO

Article history:
Received 28 October 2010
Revised 12 January 2011
Accepted 13 January 2011
Available online 19 January 2011

Keywords:
HSP90
SBDD
Virtual screening
Anticancer agents

ABSTRACT

Structure based drug design (SBDD) was used to discover heat shock protein 90 (HSP90) inhibitors useful in the treatment of cancer. By using the crystal structure of HSP90–ligand complex (1uyi), a docking model was prepared and was validated by external dataset containing known HSP90 inhibitors. This validated model was then used to virtually screen commercial databases, selected hits of which were bought and sent for real biological evaluation. Further as an alternative method, pharmacophores were generated using crystal structure conformations of ligands in HSP90 complexes (1uyi and 2bz5) and where used for virtual screening. Both cases yielded several hits containing novel scaffolds, particularly compound KHSP8 showed an IC_{50} value of 0.902 μM in case of colon cancer (HT29), which is comparable to doxorubicin (0.828 μM). These compounds were being now used as leads for constructing small molecular libraries to get compounds with favourable pharmacokinetics and drug like properties.

1. Introduction

Heat shock protein 90 (HSP90) is an ATP-dependent chaperone which belongs to ATPase/kinase super family bearing Bergerat ATP-binding fold.[1,2] HSP90 is an emerging target in cancer treatment due to its important role in maintaining transformation and in increasing the survival and growth of cancer cells.[3–7] HSP90 activity is regulated in N-terminal pocket of the protein where ATP binds and gets hydrolyzed.[3] Protein clients of HSP90 includes mostly kinases, steroid receptors and transcriptional factors involved in driving multistep malignancy and, in addition, mutated oncogenic proteins required for the transformed phenotype. Examples are Her2, Raf-1, Akt, Cdk4, cMet, mutant P53, ER, AR, mutant BRaf, Bcr-Abl, Flt-3, polo-1 kinase, HIF-1 alpha and hTERT.[5–7] Any ligands that can bind to ATP binding pocket and prevents the dissociation of HSP90 client proteins from the chaperone complex thereby the trapped proteins cannot achieve their stable conformation and are degraded by proteosome, can be of tremendous therapeutic use. Many different classes of HSP90 inhibitors were recently discovered which includes natural products like geldanamycin[8] and radicicol,[8] geldanamycin derivatives such as 17-allylamino-17-demethoxygeldanamycin (17-AAG)[9] and 17-dimethylamino-noethylamino-17-demethoxygeldanamycin (17-DMAG),[10] purine derivatives like PU3, PU24FCl and PU-H58,[11,12] pyrazoles,[13,14] naphthol,[15] quinazolinone[16] etc. 17-AAG entered clinical trials in cancer treatment but shown to have severe limitations including limited solubility, difficulties in formulation and also liver toxicity.[17] Until now, no HSP90 inhibitor is marketed as an anticancer drug and so there exits a continuous effort in the development of HSP90 inhibitors with improved pharmacological properties.

In this work we tried to use the structural knowledge of known HSP90-ligand complexes to discover new HSP90 inhibitors. Two types of methods were used for virtual screening of commercially available databases. In the first method, a docking model was generated by using FLEXX[18] program and was validated by known dataset using *C*-score. After validation the resultant model was used to screen commercial databases and hits were selected based on *C*-score. In the second method, the crystal conformations of known ligands were extracted from HSP90 complexes and by using CATALYST program[19] 3D pharmacophores were generated. The generated pharmcophores were then used to screen commercially available databases using fast-flexible search option given in CATALYST program. Hits from this step were further filtered by using FlexX docking. In both cases selected hits were subjected to real biological evaluation, which resulted in a number of novel compounds with anticancer activity. These compounds can be used as leads for further drug development.

* Corresponding author. Tel.: +82 2 958 5185; fax: +82 2 958 5189.
E-mail address: anpae@kist.re.kr (A.N. Pae).

0968-0896/$ - see front matter © 2011 Elsevier Ltd. All rights reserved.
doi:10.1016/j.bmc.2011.01.023

2. Virtual screening of HSP90 inhibitors using FlexX and *C*-score

2.1. Materials and methods

Docking model was generated using the crystal structure of HSP90 in complex with purine ligand (PDB: 1uyi). 1uyi is the crystal structure of human HSP90-alpha with 8-(2,5-dimethoxy-benzyl)-2-fluoro-9-pent-9*H*-purin-6ylamine at 2.20 Å resolution.[20] Figure 1 shows the active site of the 1uyi with purine ligand. FLEXX[18] program is used to generate the model. First single molecule docking was done to see whether the crystal conformation of the ligand is reproduced or not. The purine ligand was extracted from the crystal structure; all the atom types were checked and corrected. Hydrogens were added and the structure was minimized using Tripos force field,[21] conjugate gradient method and distance dependent dielectric constant. In the active site four conserved water molecules[22] were included and the amino acid aspartic acid 93 (ASP93) which forms hydrogen bonding with amine group of purine was kept as negative. Default volume of 6.5 Å around the ligand was considered as active site. As most of the known compounds were found to form hydrogen bonding[22] with Asp93, the oxygen of the acid group of aspartate was selected as hydrogen bond acceptor and was kept as essential using pharmaconstraints option given in FlexX. All the 30 docked poses were identical and have root mean squared (RMS) deviation of less than 1 Å indicating that the FlexX program fairly predicted the bioactive conformation of the purine ligand.

The generated model was validated by using a dataset of 58 purine ligands.[23] Figure 2 shows the different series of purine derivatives used for the validation process. The data set contains three different types of purine derivatives namely 8-arylsufanyl, 8-arylsulfoxyl and 8-arylsulfonyl adenine compounds with wide activity range of 0.03–100 μM. All the compounds of the dataset were docked in to the FlexX model and different scoring functions like *D*-score, PMF-score, *G*-score, CHEM score and *F*-score were also calculated. From these, *C*-score subset was determined by using consensus criteria of greater than or equal to three and multi function option giving equal weights to all the scores. To know which scoring function is best related with activity, correlation coefficient (r) was calculated for each of the scoring function in relation to activity data (pIC50).

Table 1 shows the r values of different scoring functions which indicates that *G*-score showed best correlation between activity and scores (r = 0.53). Figure 3 shows the graph of *G*-score values versus pIC50 clearly indicating that activity of purine ligands is increasing with increase of *G*-scores. All the active compounds

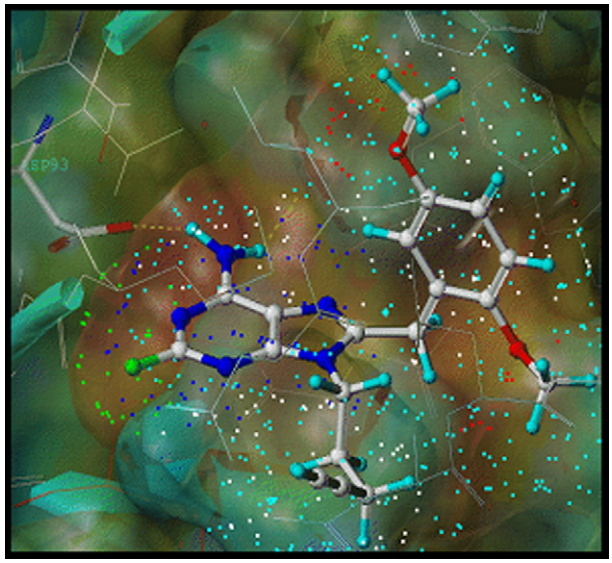

Figure 1. Active site of 1uyi with purine ligand.

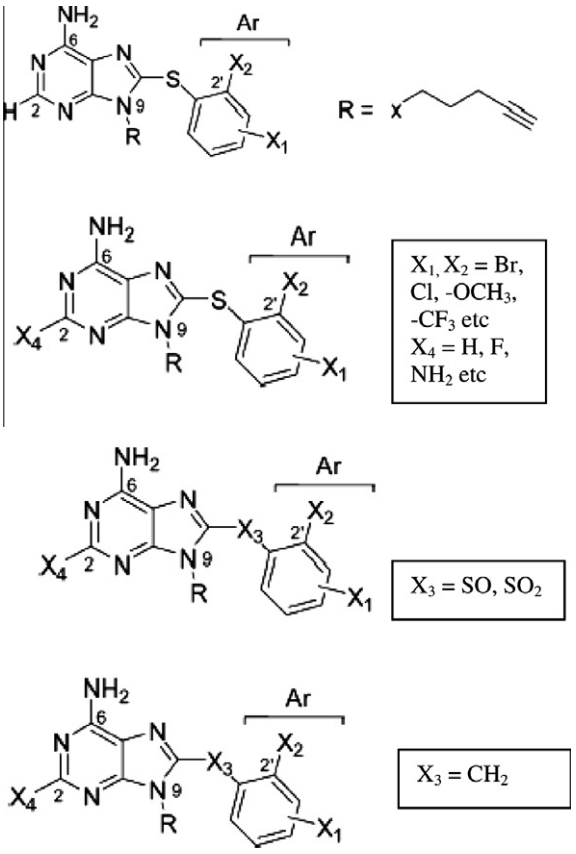

Figure 2. Purine ligands used for validation[23].

Table 1
Correlation between scoring functions and the activity (pIC_{50})

Scoring function	r
D-score	0.49
PMF-score	0.38
Chem-score	0.40
F-score	0.19
G-score	0.53

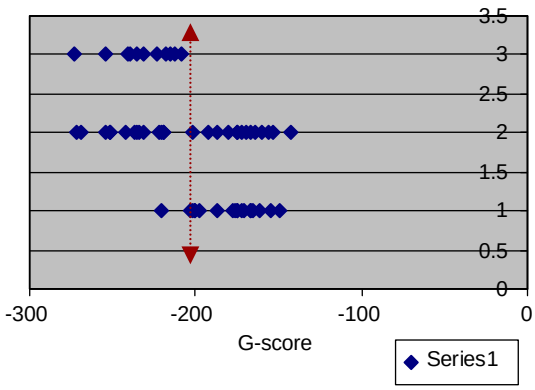

Figure 3. Graph of *G*-score versus pIC_{50}. Compounds categorized into 1, 2 and 3 based on the activities pIC_{50} 4–5: 1; pIC_{50} 5–6: 2; pIC_{50} >6: 3.

Table 2
Anticancer activity data-1 (% inhibition at 100 μM)

	A549	DU145	HT29	SK-MEL-2	SK-OV-2
HSP1	90.25	87.15	86.48	85.60	86.58
HSP2	55.83	59.94	67.90	57.12	51.62
HSP3	51.90	48.02	37.96	61.03	45.49
HSP4	51.87	40.66	64.85	58.31	34.32

A549—lung cancer; DU145—prostrate cancer; HT29—colon cancer; SK-Mel-2—malignant melanoma; SK-OV-3—ovarian cancer.

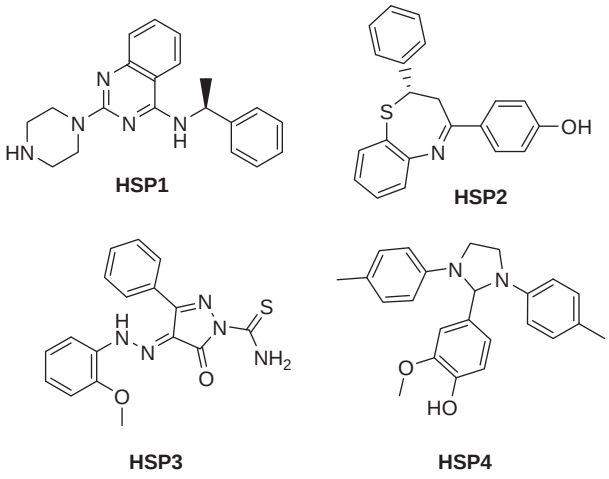

Figure 4. Structures of the HSP90 inhibitors (Table 2).

Table 3
Anticancer activity data-1 (IC_{50} values in μM)

	A549	DU145	HT29	SK-MEL-2	SK-OV-2
HSP1	13.26 ± 1.8	12.61 ± 1.2	4.10 ± 1.4	5.14 ± 0.8	14.59 ± 1.3
HSP2	33.23 ± 1.2	30.59 ± 2.5	40.73 ± 0.0	47.06 ± 1.6	61.55 ± 8.8
HSP3	45.18 ± 0.7	46.77 ± 0.0	48.48 ± 6.0	34.90 ± 4.7	76.03 ± 7.4
HSP4	27.60 ± 3.8	43.05 ± 5.3	27.63 ± 2.8	32.87 ± 4.8	>100

A549—lung cancer; DU145—prostrate cancer; HT29—colon cancer; SK-Mel-2—malignant melanoma; SK-OV-3—ovarian cancer.

with pIC_{50} more than six showed *G*-score more than −200 and compounds with pIC_{50} ranging from 4 to 5 showed *G*-score less than −200.

After validating the model and understanding that *G*-score is showing correlation with the activity in our model, commercially available Chemdiv[24] database was virtually screened using the model. 544 hits were found and from these 30 compounds were selected based on high *G*-scores and visual inspection for real biological evaluation. In these, four compounds showed more than 50% inhibition (100 μM) on one or more of the five different cancer cells tested (Table 2). Figure 4 shows the structures of these four diverse compounds which showed appreciable inhibition on cancer cells.

As a next step in biological evaluation, IC_{50} values of all these four compounds were determined. In these, compound HSP1 showed appreciable activity (Table 3).

3. Virtual screening of HSP90 inhibitors using CATALYST[19] and FLEXX

3.1. Materials and methods

In the second method, we used a novel technique, wherein three dimensional pharmacophores were generated using crystal structure conformations or bioactive conformations of ligands in known HSP90 complexes. For this purpose two HSP90 complexes, one containing purine ligand[20] (1uyi) and another containing naphthol ligand[15] (2bz5) were used. 1uyi is the crystal structure of human HSP90-alpha with 8-(2,5-dimethoxy-benzyl)-2-fluoro-9-pent-9*H*-purin-6ylamine at 2.20 Å resolution.[20] This was the same complex structure used in previous section to generate docking model. 2bz5 is the crystal structure of human HSP90-alpha with 2,5-dichloro-*N*-[4-hydroxy-3-(2-hydroxy-1-naphthyl)-phenyl]benzenesulfonamide at 1.90 Å resolution.[15] The crystal structure conformations of both the complexes were extracted and by using CATALYST program a 3D pharmacophore was generated. By observing the receptor–ligand interactions inside the active site, we can get an idea about the features that are present in the ligand and are important for binding. So by selecting these features in three dimensional space and merging them will give a hypothesis which can be used in virtual screening of commercially available databases. For example in case of 1uyi, the only direct contact of ligand with receptor is hydrogen bonding between amino group of ligand and O of carboxylate group in ASP93. Here the N of the amino group acts as donor and so this can be considered as one of the important features for binding. Other features include aromatic rings which form hydrophobic interactions with protein surface and aliphatic side chain that is exposed to solvent. These features were individually generated by defining location constraints in view hypothesis window and then all these features were merged in to one hypothesis. Figure 5 shows the pharmacophore generated by this procedure for purine ligand in 1uyi.

Similarly in case of 2bz5, the naphthalic group of the ligand acts as a hydrogen bond donor and forms hydrogen bonding with ASP93, so this can be considered as important feature and other features include hydrophobic ring systems of two phenyl and one naphthol groups. These features were also individually generated and merged as explained in previous case. Figure 6 shows the naphthol ligand of 2bz5 mapping to the generated pharmacophore. These two pharmacophores were used to screen commercially available Leadquest[25] database by using Fast-flexible search option given in CATALYST program. Virtual screening yielded 9597 and 2888 hits in case of 1uyi and 2bz5 models respectively. These hits were further reduced from 9597 to 1053 in case of 1uyi model and from 2888 to 324 in case of 2bz5 model by using the FlexX model (explained in previous section) as a secondary filtering system. This kind of filtering will aid in removing the hits that are large

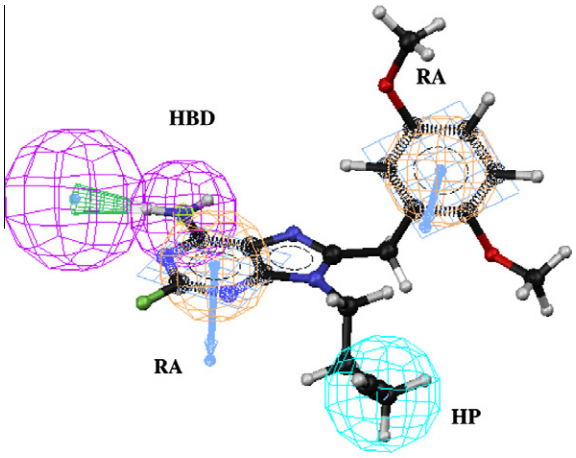

Figure 5. Purine ligand mapping to the generated pharmacophore HBD: hydrogen bond donor, HP: hydrophobic, RA: ring aromatic.

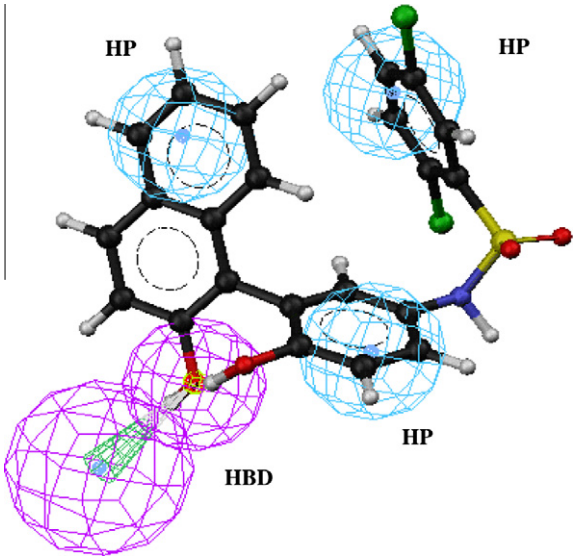

Figure 6. Naphthol ligand mapping to the generated pharmacophore HBD: hydrogen bond donor, HP: hydrophobic.

Table 4
Anticancer activity data-2 (% inhibition at 100 μM)

	A549	DU145	HT29	SK-MEL-2	SK-OV-2
HSP5	65.69	73.51	87.50	77.84	62.04
HSP6	88.78	88.67	86.11	79.50	89.50
HSP7	54.98	52.62	51.10	43.93	40.13
HSP8	43.53	44.37	63.53	33.98	22.54
HSP9	50.94	60.08	37.52	52.36	46.40
HSP10	47.86	54.53	44.63	40.10	44.05

A549—lung cancer; DU145—prostrate cancer; HT29—colon cancer; SK-Mel-2—malignant melanoma; SK-OV-3—ovarian cancer.

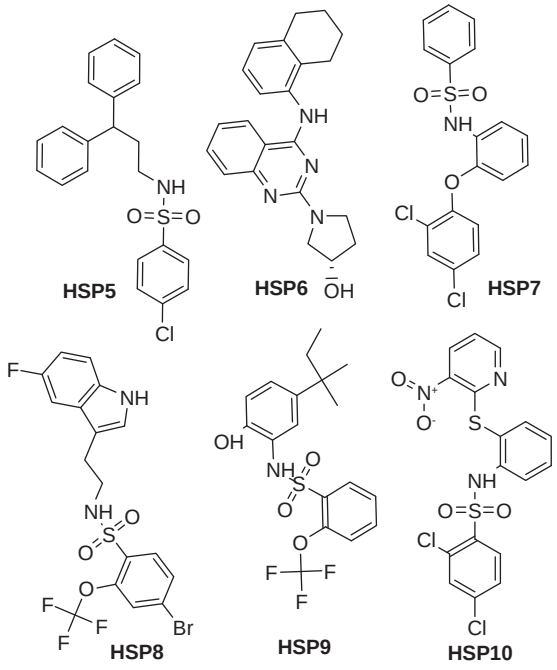

Figure 7. Structures of the HSP90 inhibitors (Table 4).

Table 5
Anticancer activity data-2 (IC_{50} values in μM)

	A549	DU145	HT29	SK-MEL-2	SK-OV-2
HSP5	30.91 ± 1.0	26.09 ± 3.9	18.83 ± 2.0	18.86 ± 1.5	35.00 ± 2.6
HSP6	12.94 ± 1.6	16.84 ± 1.9	7.12 ± 1.1	15.88 ± 1.4	16.84 ± 1.9
HSP7	35.49 ± 1.2	44.04 ± 4.7	65.08 ± 2.3	44.18 ± 2.2	>100
HSP8	54.96 ± 1.8	39.35 ± 0.6	33.38 ± 1.2	45.80 ± 5.4	>100
HSP9	38.83 ± 2.5	>100	24.10 ± 3.0	53.58 ± 4.0	38.83 ± 2.5
HSP10	26.00 ± 0.4	53.88 ± 4.3	63.11 ± 2.1	42.30 ± 6.1	69.98 ± 1.1

A549—lung cancer; DU145—prostrate cancer; HT29—colon cancer; SK-Mel-2—malignant melanoma; SK-OV-3—ovarian cancer.

or don't fit in the active site. Finally 30 compounds were selected for real biological evaluation. In these, six compounds showed more than 50% inhibition (100 μM) on one or more of the five different cancer cells tested (Table 4). Figure 7 shows the structures of these compounds.

All these six compounds were further assayed to determine IC_{50} values. In these, compound HSP6 showed appreciable activity (Table 5).

4. Results and discussion

Two types of structure based design methods were used to discover new HSP90 inhibitors. In the first one, crystal structure of 1uyi was used to generate a docking model and was subsequently used to screen commercially available Chemdiv database. In the second one, the crystal structure conformations of ligands in known HSP90–ligand complexes were extracted and were used to generate 3D pharmcophores by using CATALYST program. Both cases yielded hits showing more than 50% inhibition on one or more of the five cancer cells tested. Out of these, two compounds namely HSP1 and HSP6 showed appreciable IC_{50} values (Table 6).

Figure 8 shows the structures of both HSP1 and HSP6. From the structures it is striking to observe that they are very similar, even though they are obtained from completely different methods and are from different databases. HSP1 is obtained from Chemdiv[24] database and HSP6 is obtained from Leadquest[25] database. Chemically HSP1 is *N*-((*S*)-1-phenylethyl)-2-(piperazin-1-yl) quinazolin-4-amine and HSP6 is (*S*)-1-(4-(1,2,3,4-tetrahydronaphthalen-5-ylamino)quinazolin-2-yl) pyrrolidin-3-ol. Both are quinazoline compounds with hydrogen bond donor part in HSP1 is occupied by NH of piperazine moiety and in HSP6 it is

Table 6
Anticancer activity data of the most active compounds (IC_{50} values in μM)

	A549	DU145	HT29	SK-MEL-2	SK-OV-2
Hsp1	13.26 ± 1.8	12.61 ± 1.2	4.10 ± 1.4	5.14 ± 0.8	14.59 ± 1.3
Hsp6	12.94 ± 1.6	16.84 ± 1.9	7.12 ± 1.1	15.88 ± 1.4	16.84 ± 1.9

A549—lung cancer; DU145—prostrate cancer; HT29—colon cancer; SK-Mel-2—malignant melanoma; SK-OV-3—ovarian cancer.

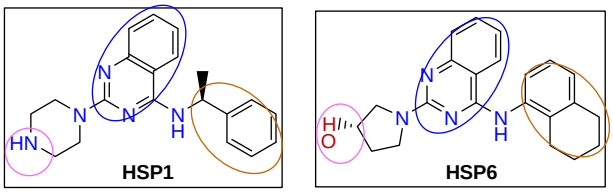

Figure 8. Structures of HSP1 and HSP6 with similar features.

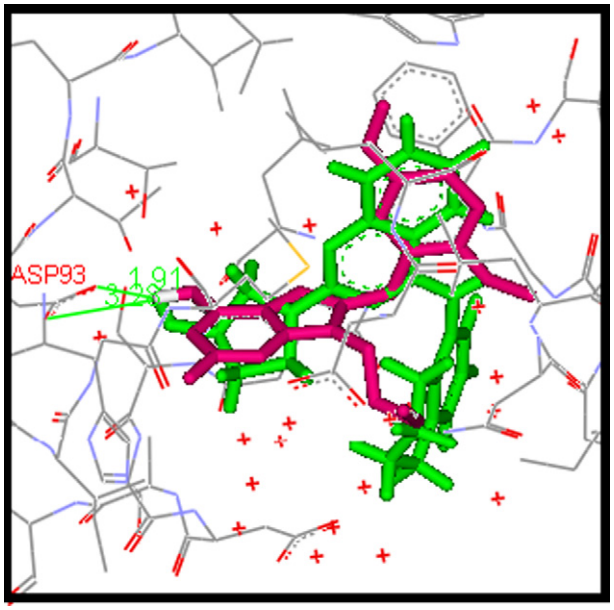

Figure 9. HSP6 docked in 1uyi active site; Green: HSP6; Pink: purine ligand.

occupied by OH at 3-position in pyrrolidine moiety. The solvent exposed hydrophobic portion is occupied by phenylethanamine and tetrahydonaphthalene moieties in case of HSP1 and HSP6, respectively.

To observe receptor-interactions of these compounds, one of the positive hit, HSP6 is docked in to active site of 1uyi. Figure 9 shows the overlap of HSP6 on purine ligand in the active site of 1uyi. In the figure purine ligand is shown in pink and HSP6 is shown in green. We can observe that OH group of pyrrolidine group forming hydrogen bond with ASP93. The distances between the OH group and the two oxygens of carboxylate group of ASP93 were also shown (1.91 Å and 3.28 Å). The 1-pentynyl group of purine ligand exposed to solvent is overlapped with tetrahydronaphthalene moiety of HSP6.

Table 7
Anticancer activity data of the similar compounds (% inhibition at 100 μM)

	DU145		HT29		SK-Mel-2	
	100 μM	100 μM	100 μM	100 μM	100 μM	100 μM
KHSP1	93.38	38.16	89.90	74.36	91.26	69.86
KHSP2	92.93	52.21	89.28	80.65	92.33	81.16
KHSP3	92.86	57.95	88.05	83.27	91.82	91.58
KHSP4	93.62	53.74	78.71	77.87	93.32	77.62
KHSP5	93.38	86.54	89.62	89.82	92.34	91.48
KHSP6	81.89	35.04	78.93	61.28	85.45	46.74
KHSP7	93.26	30.31	86.18	67.59	92.30	38.95
KHSP8	90.86	28.70	89.34	64.20	92.53	22.81

DU145—prostrate cancer; HT29—colon cancer; SK-Mel-2—malignant melanoma.

Parent Chemdiv database was further searched for compounds similar to HSP1 and HSP6. Recently it was proposed[16] that in case of quinazolinone compounds, the interaction between ASP93 and ligand can also be possible by means of a water molecule. For that reason we tried to select similar compounds containing both hydrogen bond donor and acceptor moieties to understand structure activity relationships of quinazoline compounds in relation to HSP90 inhibitory activity. Forty of the selected compounds were bought from the Chemdiv and tested for anticancer activity. In

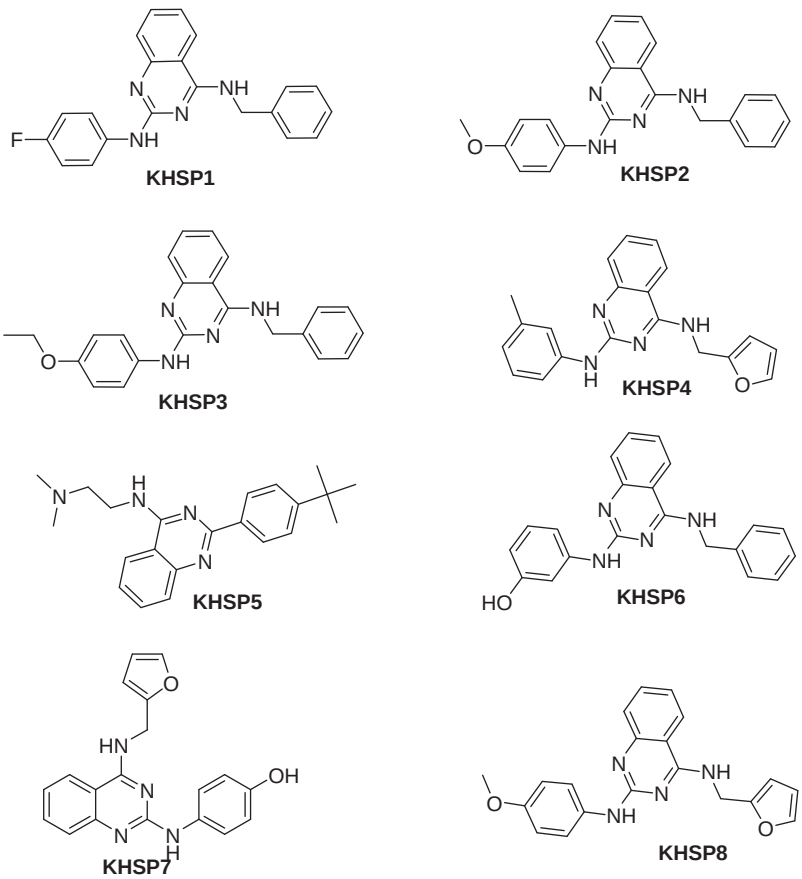

Figure 10. Structures of the HSP90 inhibitors (Table 7).

Table 8
Anticancer activity data of the similar compounds (IC_{50} values in μM)

	DU145	HT29
KHSP1	23.39 ± 8.3	2.41 ± 0.1
KHSP2	21.30 ± 3.1	13.40 ± 2.2
KHSP3	19.17 ± 4.7	16.47 ± 3.1
KHSP4	19.65 ± 3.6	10.06 ± 3.3
KHSP5	>50	8.72 ± 3.4
KHSP6	22.60 ± 1.3	15.83 ± 1.2
KHSP7	22.69 ± 10.3	14.03 ± 1.1
KHSP8	24.53 ± 4.4	0.902 ± 0.92

DU145—prostrate cancer; HT29—colon cancer.

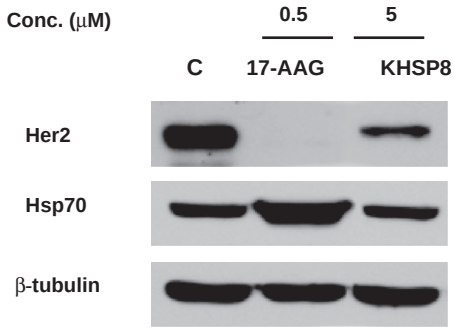

Figure 11. Effects of KHSP8 on Her2 degradation and HSP70 induction. MCF-7 cells were treated with 17-AAG (0.5 μM) and KHSP8 (5 μM) and solvent as 0.4% DMSO. Tubulin was used as loading control.

these compounds some of them showed appreciable inhibition on all three of the cancer cells tested both at 100 and 10 μM concentrations (Table 7). Figure 10 shows the structures of these compounds. KHSP6 and KHSP7 have hydrogen bond donor group to form hydrogen bonding with ASP93. All other don't have donor group in that specific position indicating that presence of hydrogen bond donor may be not compulsory for activity. These compounds were further assayed to determine IC_{50} values (Table 8).

All the compounds showed appreciable IC_{50} values on one or both of the DU145 and HT29 cancer cells tested. KHSP8 showed very high anticancer activity of about 0.902 μM in case of colon cancer (HT29) which is comparable to doxorubicin (0.828 μM). Further to ascertain that whether this anticancer activity is truly due to HSP90 inhibition, KHSP8 was tested for its effect on her2 degradation (one of the HSP90 client proteins) and HSP70 induction in MCF-7 breast cancer cell line (Fig. 11). KHSP8 effectively inhibited the growth of MCF-7 cells with IC_{50} value of 7.25 μM in MTT assay. For this reason we thought this compound as ideal for using as lead for further development of HSP90 inhibitors. Construction of small molecule libraries based on the structure of KHSP8 to yield compounds with favorable pharmacokinetic properties is already in progress and results will be published soon.

5. Assay methods

5.1. MTT assay

Cytotoxic activity of the anticancer drugs against human cancer cell lines was investigated using the MTT assay. Human lung cancer (A549), Human colon cinomadenocara (HT-29), Human prostate cancer (DU145), human ovarian cancer (SKOV3) and human melanoma cancer cell lines (SKMEL2) were obtained from the Korean Cell Line Bank, Seoul National University. All cell lines were grown in RPMI 1640 (Gibco BRL) supplemented with 10% (V/V) heat inactivated Fetal Bovine Serum (FBS) and maintained at 37 °C in a humidified atmosphere with 5% CO_2. The cells (3×10^3 cells/well) were seeded into 96-well plate. Various concentrations of samples was added to each well in duplicate, and then incubated at 37 °C with 5% CO_2 for 2 days such that the cells are in the exponential phase of growth at the time of drug addition. After that 15 μl of the Dye solution (Promega, CellTiter96) was added to each well. The plate was incubated at 37 °C for up to 4 h in a humidified 5% CO_2 atmosphere. After incubation, 100 μl of the Solubilization solution/StopMix (Promega, CellTiter96) was added to each well. Then the plate was allowed to stand overnight in a sealed container with a humidified atmosphere at room temperature to completely solubilize the formazan crystals. The optical density was measured using a microplate reader (Versamax, Molecular Devices) at 570 nm wavelength and the anticancer effective concentration was expressed as GI_{50}.

5.2. Her2 degradation assay

MCF-7 cells were seeded into 6-well plates at a density of 10^5 cells/well and grown upto 60% confluency. Grown cells were treated with the compounds, 17-AAG which were dissolved in DMSO, or DMSO alone as a control. Cells were incubated for additional 24 h, then harvested, lysed in TNES buffer [50 mM Tris–HCl, pH 7.4, 1% NP-40, 2 mM EDTA, 100 mM NaCl, 1 mM PMSF, 0.1% protease inhibitor cocktail solution]. The clarified cell lysates were collected after centrifugation and the protein concentration of each lysates were determined by Protein assay solution (Bio-rad). Each lysates containing 50 μg of total protein was loaded, subjected to SDS–PAGE and transferred to nitrocellulose membrane. After probed with antibody against Her2-neu (Santa Cruz Biotechnology), the membrane was stripped and also probed with antibodies against β-tubulin (Santa Cruz Biotechnology) and Hsp70 (Stressgen Bioreagents), respectively.

Acknowledgments

This work is supported by Korea Science and Engineering Foundation (KOSEF) and Korea Institute of Science and Technology (KIST).

References and notes

1. Dutta, R.; Inouye, M. *Trends Biochem. Sci.* **2000**, *25*, 24.
2. Terasawa, K.; Minami, M.; Minami, Y. *J. Biochem.* **2005**, *137*, 443.
3. Wegele, H.; Muller, L.; Buchner, J. *Rev. Physiol. Biochem. Pharmacol.* **2004**, *151*, 1.
4. Mosser, D. D.; Morimoto, R. I. *Oncogene* **2004**, *23*, 2907.
5. Kamal, A.; Boehm, M. F.; Burrows, F. J. *Trends Mol. Med.* **2004**, *10*, 283.
6. Neckers, L. *Trends Mol. Med.* **2002**, *8*, S55.
7. Maloney, A.; Workman, P. *Exp. Opin. Biol. Ther.* **2002**, *2*, 3.
8. Roe, S. M.; Prodromou, C.; O'Brien, R.; Ladbury, J. E.; Piper, P. W.; Pearl, L. H. *J. Med. Chem.* **1999**, *42*, 260.
9. Schulte, T. W.; Neckers, L. M. *Cancer Chemother. Pharmacol.* **1998**, *42*, 273.
10. Egorin, M. J.; Lagattuta, T. F.; Hamburger, D. R.; Covey, J. M.; White, K. D.; Musser, S. M.; Eiseman, J. L. *Cancer Chemother. Pharmacol.* **2002**, *49*, 7.
11. Chiosis, G.; Lucas, B.; Shtil, A.; Huezo, H.; Rosen, N. *Bioorg. Med. Chem.* **2002**, *10*, 3555.
12. He, H. Z.; Zatorska, D.; Kim, J.; Aguirre, J.; Llauger, L.; She, Y. H.; Wu, N.; Immormino, R. M.; Gewirth, D. T.; Chiosis, G. *J. Med. Chem.* **2006**, *49*, 381.
13. Cheung, K. M. J.; Matthews, T. P.; James, K.; Rowlands, M. G.; Boxall, K. J.; Sharp, S. Y.; Maloney, A.; Roe, S. M.; Prodromou, C.; Pearl, L. H.; Aherne, G. W.; McDonald, E.; Workman, P. *Bioorg. Med. Chem. Lett.* **2005**, *15*, 3338.
14. McDonald, E.; Jones, K.; Brough, P. A.; Drysdale, M. J.; Workman, P. *Curr. Top. Med. Chem.* **2006**, *6*, 1193.
15. Barril, X.; Brough, P.; Drysdale, M.; Hubbard, R. E.; Massey, A.; Surgenor, A.; Wright, L. *Bioorg. Med. Chem. Lett.* **2005**, *15*, 5187.
16. Park, H.; Kim, Y. J.; Hahn, J. S. *Bioorg. Med. Chem. Lett.* **2007**, *17*, 6345.
17. Jia, W. T.; Yu, C. R.; Rahmani, M.; Krystal, G.; Sausville, E. A.; Dent, P.; Grant, S. *Blood* **2003**, *102*, 1824.

18. Rarey, M.; Kramer, B.; Lengauer, T.; Klebe, G. *J. Mol. Biol.* **1996**, *261*, 470.
19. CATALYST 4.11 (software package): San Diego, CA; Accelrys, 2005.
20. Wright, L.; Barril, X.; Dymock, B.; Drysdale, M.; Surgenor, A.; Sheridan, L.; Beswick, M.; Collier, A.; Massey, A.; Fromont, C.; Davies, N.; Sharp, S.; Workman, P.; Hubbard, R. E. *Clin. Cancer Res.* **2003**, *9*, 6070s.
21. SYBYL 6.9. Tripos Inc., 1699 Hanley Road, St. Louis, MO 63144.
22. Wright, L.; Barril, X.; Dymock, B.; Sheridan, L.; Surgenor, A.; Beswick, M.; Drysdale, M.; Collier, A.; Massey, A.; Davies, N.; Fink, A.; Fromont, C.; Aherne, W.; Boxall, K.; Sharp, S.; Workman, P.; Hubbard, R. E. *Chem. Biol.* **2004**, *11*, 775.
23. Llauger, L.; He, H. Z.; Kim, J.; Aguirre, J.; Rosen, N.; Peters, U.; Davies, P.; Chiosis, G. *J. Med. Chem.* **2005**, *48*, 2892.
24. <http://www.chemdiv.com/>.
25. <http://www.tripos.com/>.